GEOPHYSICAL RESEARCH LETTERS, VOL. ???, XXXX, DOI:10.1029/,

Impact of interactive aerosol on the African Easterly Jet in the NASA GEOS-5 global forecasting system.

O. Reale,[1,2] K. M. Lau,[1] A. da Silva[3]

O. Reale, Laboratory for Atmospheres, Code 613, NASA Goddard Space Flight Center, Greenbelt, MD 20771, USA. (Oreste.Reale-1@nasa.gov)

[1]NASA Goddard Space Flight Center, Laboratory for Atmospheres, Greenbelt, Maryland, USA.

[2]University of Maryland, Baltimore County, Baltimore, Maryland, USA.

[3]NASA Goddard Space Flight Center, Global Modeling and Assimilation Office, Maryland, USA.

The real-time treatment of interactive, realistically varying aerosol in a global operational forecasting system, as opposed to prescribed (fixed or climatologically varying) aerosols, is a very difficult challenge that only recently begins to be addressed. Experiment results from a recent version of the NASA GEOS-5 forecasting system, inclusive of interactive aerosol treatment, are presented in this work. Four sets of 30 5-day forecasts are initialized from a high quality set of analyses previously produced and documented, to cover the period from 15 August to 16 September 2006, which corresponds to the NASA African Monsoon Multidisciplinary Analysis (NAMMA) observing campaign. The four forecast sets are at two different horizontal resolutions and with and without interactive aerosol treatment. The net impact of aerosol, at times in which there is a strong dust outbreak, is a temperature increase at the dust level, and decrease in the near-surface levels, in complete agreement with previous observational and modeling studies. Moreover, forecasts in which interactive aerosols are included depict an African Easterly Jet at slightly higher elevation, and slightly displaced northward, with respect to the forecasts in which aerosols are not included. The shift in the AEJ position goes in the direction of observations and agrees with previous results.

1. Introduction

The role of the Saharan Air Layer (SAL) has been suggested to be relevant to weather forecasting over the tropical Atlantic since at least the early '70s [Carlson and Prospero, 1972]. In addition to the thermal effect due to its intrinsically high heat content, the role of dust in terms of direct radiative effect has been intensely investigated for several decades (e.g., Carlson and Benjamin, [1980]). Surface- and space-based measurements of atmospheric optical thickness (AOT) go back to the late '70s (e.g. [Carlson and Wendling, 1977]) but the possibilities of merging modern-era satellites with data such as the ones coming from Moderate Resolution Imaging Spectroradiometer (MODIS) or Cloud-Aerosol Lidar and Infrared Pathfinder Satellite Observation (CALIPSO) give a much more accurate understanding of aerosols' optical properties (e.g. [Remer et al. 2008; Omar et al. 2009])

Among the various effects of dust over the tropical atmosphere, Dunion and Velden [2003] suggested a role of dust unfavorable to tropical cyclogenesis. One point of their argument, among other issues, is the increased static stability induced by mid-troposphere warming and surface cooling. Similar findings are also obtained by Lau and Kim [2007] on a seasonal time-scale. Reale et al. [2009b], hereafter RA09b, relying upon a global data assimilation and modeling effort and the production of high quality analyses, also suggest that high dust content is associated with a thermal dipole: relatively warm at 600-700 hPa and cooler at about 900 hPa or below. RA09b findings are supported by the fact that the finite-volume dynamics of the NASA GEOS-5 is particular suitable to maintain fine thermal features avoiding unrealistic dispersions.

Recent climate sensitivity experiments using general circulation models have shown that radiative effects of Saharan dust tend to draw the Atlantic ITCZ northward towards the southern edge of the dust layer, and induce large-scale north-south and east-west oriented divergent circulations that affect the African Easterly Waves and rainfall variability of the West African monsoon and climate of the Atlantic [Lau et al., 2009; Kim et al.; 2010]. Wilcox et al. [2010] have shown from observational perspective that the temperature structure associated with Saharan air outbreaks is consistent with previous work, and that one of the effects of dust outbreaks is a northward shift of the Inter Tropical Convergence Zone (ITCZ). Also within the operational forecasting modeling framework, evidence has been provided by Tompkins et al. [2005] on that an improved representation of aerosol (i.e. seasonally varying instead of fixed) leads to a more correct representation of the African Easterly Jet (namely, a northward and upward shift, in agreement with observations).

In this work, the use of interactive aerosol in a global modeling framework provides results fully consistent with Lau et al. [2009], Kim et al. [2010], Wilcox et al. [2010] and confirms that the direction started by the pioneering work by Tompkins et al. [2005] needs to be further pursued.

2. The Model and Data Assimilation System

The global data assimilation and forecasting system used is the NASA GEOS-5, which combines the Gridpoint Statistical Interpolation (GSI) analysis algorithm developed by the National Centers for Environmental Predictions (NCEP) (e.g. Wu et al., [2002]), and modified by the NASA Global Modeling Assimilation Office (GMAO), with the NASA atmospheric global forecast model, is documented in Rienecker et al., [2008]. The fore-

cast model shares the same dynamical core [Lin, 2004] with the so-called finite-volume General Circulation Model (fvGCM), also known as the GEOS-4, but contains a different set of physical parametrizations, partly developed by the NASA GMAO. The Aerosol interactive component is a new feature which is currently implemented also in the operational version of the GEOS-5 and is a further step with respect to the previous transport model described in Colarco et al. [2010], which merged the Goddard Chemistry, Aerosol, Radiation and Transport Model (GOCART) with the GEOS-4. The version described by Colarco et al. [2010] allows the treatment of dust, sea salt, carbonaceous and sulfate aerosols, producing realistic aerosol distributions (validated against ground- and satellite-based measurements) which are consistent with the dynamics and the meteorological fields produced by the GEOS-4. In the version used in this study, aerosol transport processes (advection, diffusion, convection) are provided by the host GEOS-5 model, with the aerosol specific processes (emission, deposition, simplified sulfate chemistry) as in Colarco et al. [2010]. The direct aerosol radiative effect is included in the GEOS-5, while indirect effects on cloud/precipitation processes are not included at present.

3. The Experiments

Four sets of 30 5-day forecast experiments at two horizontal resolutions ($0.5^o \times 0.67^o$ and $0.25^o \times 0.33^o$, both with 72 vertical levels), are performed. They are initialized daily at 00z, starting at 00z 15 August 2006, from the same set of analyses used in RA09b. These were produced by assimilating all conventional and satellite observations used operationally at that time, but with a much denser coverage from the Atmospheric Infrared Sounder (AIRS), obtained by ingesting cloudy retrievals instead of clear-sky

radiances. As discussed in Reale et al. [2009a] and in RA09b, AIRS-derived information in partly cloudy regions improves the analyses in the tropics. However, the experiments described in this article are characterized by the inclusion or exclusion of interactive aerosol, and are named NOA_{xx} (no aerosol) and IAA_{xx} (interactive aerosol) with the suffix $_{xx}$ indicating the 0.50^o or 0.25^o forecasts respectively.

4. Results

As a preliminary metric to assess the impact of interactive aerosol, the anomaly correlation for all sets of 30 5-day forecasts is computed against operational NCEP analyses. The impact is virtually zero: the insertion of interactive aerosol does not affect the *globally averaged* skill of the system. In FS1 the anomaly correlations of NOA_{50} and IAA_{50} are compared; the 0.25^o forecasts provide identical results (not shown). The lack of global impact of the interactive aerosol is understandable because the production of dust is confined to few areas of the world, and does not occur at all times even in the dust-producing regions. However, it is important to notice that the forecast skill does not degrade as a consequence of the insertion of aerosols, which represents a major change in the model's physics.

At the same time, it is crucial to emphasize that, for states of the atmospheres associated with *specific* weather systems, at times in which dust production is strong, and selected regions are analyzed, the impact of aerosol insertion is very large and dynamically relevant. In this work we focus on the impact on the African Easterly Jet (AEJ) which flows, with a predominantly easterly component, at about 650 hPa and about $15^o - 20^oN$, and which is partly controlled by horizontal temperature gradients over the Sahelian region.

To detect and understand the impact of interactive aerosols is not an easy or obvious task, because of the intrinsically noisy nature of the radiative forcing associated with dust, the overlapping with strong thermal signal due to the diurnal cycle, and finally the inhomogeneous distribution of dust, rapidly varying in space and time. In this work, we aim to show an example of a clear signal associated to a major dust outbreak. We select the strong outbreak observed during the Special Observing Phase (SOP-3) of NAMMA, moving from Africa to the Atlantic between 25 and 28 August. RA09b suggest that this event produced a temperature dipole (cool at about 900 hPa and warm at about 600 hPa), whose effect propagated well into the Atlantic. However, RA09b did not have yet the capability of interactive aerosol and is based on a comparison between the MODIS AODs, and on the temperature structure in the GEOS-5 analyses and integrations [Reale and Lau 2010]. In this work we rediscuss the presence of a thermal dipole possibly associated with dust, in lieu of this new NASA tool.

As a first step, it is important to verify that the above-referred dust outbreak is represented well in the simulations. Figure 1 compares the outbreak as represented through the total mass column dust obtained from the 36-hour GEOS-5 forecast initialized at 00z 24 August, and a composition of AOTs obtained from MODIS instruments on board both Aqua and Terra satellites, corresponding to the verification time of 12z 25 August. The Figure shows that the GEOS-5 reproduces a strong dust outbreak intercepting the African coastline at about $20^o - 30^oN$, recurving southward at about 20^oW and northwestward at about $25^oW - 35^oW$.

Figure FS2 shows the same outbreak, as captured by a 36-hour forecast initialized on the following day, at 00z 25 August 2006. By comparing the observed AOD from 12z 26 August with the forecast, it can be seen that GEOS-5 again captures well the westward propagation of the dust edge, and even produces a very thin low-dust channel between the two major high dust regions centered at about 15^oN, $30-40^oW$ and 25^oN, $20-30^oW$, respectively. On these grounds, it can be safely stated that there is a major dust outbreak in the GEOS-5, and that its timing and scale correspond well with the MODIS data.

The second step is to investigate the impact of this dust outbreak on the temperature structure, as represented by the GEOS-5. Figure 2 shows the temperature impact of aerosols at longitude 10^oW, from the same simulations in Fig. 1. An evident strong thermal dipole, very similar to the one discussed in RA09b and previously by Dunion and Velden [2004] can be observed: a heating of about $1^oC-1.5^oC$ between 850 and 500 hPa, and a cooling in the lower, near-surface, levels. A very similar pattern in the IAA_{25} minus NOA_{25} temperature structure across the same latitude range and at longitude 10^oW can be seen also in FS 3, where the corresponding aerosol impact on temperature is computed from the 36 hour forecast initialized on the following day (00z 25 August) and verified at 12z 26 August. The simulations at 0.50^o provide consistent results (not shown) but with diluted values and smoother gradients. As discussed in RA09b and Reale and Lau (2010), the resolution of 0.25^o is better than 0.50^o to investigate the fine structure of the AEJ. For this reason, we show only the IAA_{25} in the following pictures.

Because the AEJ and the wind over the region are strongly controlled by lower-level temperature gradients, a change in the thermal structure must have an impact on the

AEJ and more generally on the circulation. Figure 3 shows the vertical profiles extracted from a 108 hour forecast in the GEOS-5 integrations (NOA_{25} and IAA_{25}) and compared with the profiles of temperature and zonal wind component, obtained from the vertical ground-based soundings from the Cape Verde Islands, at $14.9^oN, 23.5^oW$ (radiosonde data available online at: http://namma.nsfc.nasa.gov). The most evident impact on temperature is a warming up to 1^oC between 900 and 700 hPa, and a slight cooling from the near-surface levels up to 900 hPa. The zonal wind panel shows that the verifying analysis and the observational profile match very well, but the 108 hour NOA_{25} forecast has a negative bias with respect to the observations, of about $4ms^{-1}$, from the surface to 800hPa. The impact of the aerosol is very evident in the lower levels, reducing the bias of about 40%. When no dust production is present, the impact on temperature and zonal wind is negligible (not shown). Also, above 600hPa, the impact of the aerosol is virtually zero (not shown).

The radiative effect of dust is controlled by diurnal cycle and the distribution of aerosol is very noisy; therefore, to obtain a clearer signal on the wind field and of the AEJ structure, a 5-day average across the forecast initialized on August 25th is performed. There is an evident northward and upward shift in the AEJ structure, in the zonal wind and temperature fields at 10^oW (FS 4) consequent to this thermal anomaly, in agreement with Tompkins et al. [2005], and expected from the thermal wind relationship. We see a similar thermal anomaly at 10^oE and a corresponding northward shift in the AEJ (FS 5). The shift is also very evident on any longitude between 20^oW and 20^oE (not shown) and, to a lesser extent, also in the IAA_{50} experiments (not shown). The scarcity

of observations from the area (which prevents from providing a clear depiction of the AEJ from observations only) does not allow the validation of this northward shift in a more rigorous way. To compare the AEJ with reanalyses is also not meaningful since no reanalysis is produced from a system containing realistic, interactive aerosol at this time. However, these experiments demonstrate that the effect of interactive aerosol in the model, without degrading the global forecasting skill, alter significantly the circulation over the dust-affected region and provide an improved vertical profile at one validation point.

5. Discussion

The introduction of interactive aerosol, varying in agreement with the meteorology, is a serious challenge requiring consideration. In this work it is shown that the usual metrics to asses improvement in forecasting skill, such as 500 hPa anomaly correlation plots, are not suitable to evaluate the impact of the insertion of interactive aerosol treatment. On the contrary, for areas and events affected by dust aerosols, it is important to design meaningful, event-focused, metrics. In this work a major dust outbreak observed during the NAMMA campaign in August 2006 is investigated with the aid of the GEOS-5 forecasting system inclusive of interactive aerosol component. It is first shown that the forecast of dust total column mass qualitatively agrees with the MODIS merged AOTs from both Aqua and Terra, and then that the effect of the aerosol on the temperature structure is completely consistent with previous observational and modeling works, producing a thermal dipole (warmer at the aerosol level, cooler below). In particular, it is shown that the effect of this thermal anomaly projects into the dynamics and produces an improved 108

hour forecast of temperature and wind profiles, validated against an existing sounding. A 5-day average across the forecast, to dampen the noisy structure of the dust-induces signal, shows that the net effect of the aerosol simulation is a northward (and, to a lesser extent, upward) shift of the AEJ, in agreement with other modeling studies. FS 4 and 5 also suggest a northward displacement of the westerly low-level monsoonal flow, in agreement with Wilcox et al. [2010] and related modeling results [e.g. Lau et al 2009]. In this work we have also performed the same analysis for another dust outbreak occurred around 10-13 September: wind and temperature anomalies of the same sign are obtained, albeit of a weaker magnitude, being the outbreak also substantially weaker (not shown).

6. Concluding Remarks

In this article we show that the use of interactive aerosol in the GEOS-5 data assimilation and forecasting system does not impact the global skill but substantially changes the thermal structure over northwestern tropical Africa, during an observed dust outbreak, affecting the circulation and particularly the AEJ representation. We validate the changes in temperature and wind with a vertical sounding, showing that the insertion of interactive aerosol improves the forecast up to day five for this particular event. However, the limitation of this work is to rely upon modeled aerosol production and distribution. The next step, namely real-time use of satellite-derived aerosol information in global models, is a very recent development of the most advanced data assimilation systems. In this regard, the NASA GMAO is currently attempting to assimilate real-time AOTs from MODIS, which may represent the future direction for this kind of research.

Acknowledgments. The authors thank Dr. Ramesh Kakar for support through grant NAMMA and Dr. Tsengdar Lee for allocations on NASA High-End Computing systems.

References

Carlson, T. N. and J. M. Prospero, (1972), The large-scale movement of Saharan air outbreaks over the northern equatorial Atlantic. *J. Appl. Meteor., 11* 283-297.

Carlson, T. N. and P. Wendling, (1977), Reflected radiance measured by NOAA 3 VHRR as a function of optical depth for Saharan dust. J. Appl. Meteor., 16, 1368-1371.

Carlson T. N., and S. G. Benjamin, (1980), Radiative heating rates for Saharan dust. *J. Atmos. Sci., 37*, 193213.

Colarco, P., A. da Silva, M. Chin, and T. Diehl, (2010) Online simulations of global aerosol distributions in the NASA GEOS-4 model and comparison to satellite and ground-based aerosol optical depth. *J. Geophys. Res, in press.*

Dunion, J., and C. S. Velden, 2004: The impact of the Saharan Air Layer on Atlantic Tropical Cyclone activity. *Bull. Am. Meteorol. Soc., 85, 353-365.*

Kim, K.-M., K. M. Lau, Y. C. Sud, and G. Walker, (2010): Influence of aerosol-radiative forcings on the diurnal and seasonal cycles of rainfall over West Africa and Eastern Atlantic Ocean using GCM simulations. *Clim. Dyn.*, doi: 10.1007/s00382-010-0750-1.

Lau, K. M., and K.-M. Kim, (2007), How nature foiled the 2006 hurricane forecasts, EOS, Trans. Amer. Geophys. Union, 88, 105-17.

Lau, K. M., Kim, K. M., Sud, Y. C., Walker, G. K., 2009: A GCM study of the response of the atmospheric water cycle of West Africa and the Atlantic to Saharan dust radiative forcing. *Ann. Geophys. 27*, 4023-4037.

Lin, S.-J., 2004: A 'vertically lagrangian' finite-volume dynamical core for global models. *Mon. Wea. Rev., 132*, 2293-2307.

Omar, A. H., and co-authors, (2009), The CALIPSO automated aerosol classification and lidar ratio selection algorithm *J. Atmos. Oceanic Technol., 26*, 19942014.

Reale, O., J. Susskind, R. Rosenberg, E. Brin, E. Liu, L. P. Riishojgaard, J. Terry, J. C. Jusem, (2008), Improving forecast skill by assimilation of quality-controlled AIRS temperature retrievals under partially cloudy conditions. *Geophys. Res. Lett., 35*, L08809, doi:10.1029/2007GL033002.

Reale, O., W. K. Lau, J. Susskind, E. Brin, E. Liu, L. P. Riishojgaard, M. Fuentes, R. Rosenberg, (2009), AIRS Impact on the Analysis and Forecast Track of Tropical Cyclone Nargis in a global data assimilation and forecasting system. *Geophys. Res. Lett., 36*, L06812, doi:10.1029/2008GL037122.

Reale, O., W. K. Lau, K.-M. Kim, E. Brin, (2009), Atlantic tropical cyclogenetic processes during SOP-3 NAMMA in the GEOS-5 global data assimilation and forecast system. *J. Atmosph. Sci.*, **66,** 3563-3578.

Reale, O., and W. K. Lau, (2010), Reply. *J. Atmosph. Sci., 67*, 24112415.

Remer and co-authors, (2008), Global aerosol climatology from the MODIS satellite sensors, *J. Geophys. Res., 113*, D14S07, doi:10.1029/2007JD009661.

Rienecker, and co-authors (2008), The GEOS-5 Data Assimilation System. Documentation Versions 5.0.1, 5.1.0 and 5.20 *Technical Report Series on Global Modeling and Data Assimilation*, **27**, NASA/TM-2008-104606, 1-118, Available online at: http://gmao.gsfc.nasa.gov/pubs/tm/

Tompkins, A. M., C. Cardinali, J.-J. Morcrette, and M. Rodwell, (2005), Influence of aerosol climatology on forecasts of the African Easterly Jet, *Geophys. Res. Letter.*, *32*, L10801, doi:10.1029/2004GL022189.

Wilcox, E. M., K. M. Lau, and K.-M. Kim, (2010) A northward shift of the north Atlantic Ocean Inter-tropical Convergence Zone in response to summertime Saharan Dust Outbreaks, *Geophys. Res. Lett.*, *37*, doi:10.1029/2009GL041774.

Wu, W.-S., R.J. Purser and D.F. Parrish, (2002), Three-dimensional variational analysis with spatially inhomogeneous covariances, *Mon. Wea. Rev.*, *130*, 2905-2916.

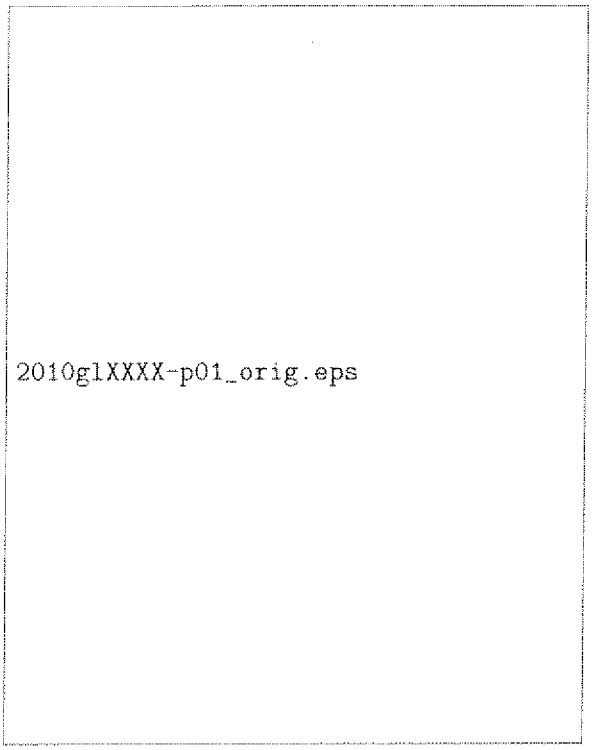

Figure 1. 36-hour forecast (initialized at 00z 24 Aug 2006) of total mass column aerosol from the GEOS-5, and MODIS optical depth for 12z 25 Aug 2006.

Figure 2. Vertical Meridional cross-section of temperature (^oC) at 10^oW in the GEOS-5 NOA_{25} simulation for 12z 25 Aug 2006, (36 hour forecast, initialized at 00z 24 Aug). Shaded: IAA_{25} minus NOA_{25} difference.

Figure 3. Vertical profiles of Temperature (^oC, left panel) and zonal wind u (ms^{-1}, right panel) at Cape Verde $14.92^oN, 23.49^oW$ in the GEOS-5 NOA_{25} (green) simulation for 12z 29 Aug 2006, (108 hour forecast, initialized at 00z 25 Aug), verifying analyses (black), compared with observed soundings (purple) at the Cape Verde, from SOP-3 campaign. In the left panel the orange line represents the IAA_{25} minus NOA_{25} difference; in the right panel, the actual IAA_{25} u component of the wind.

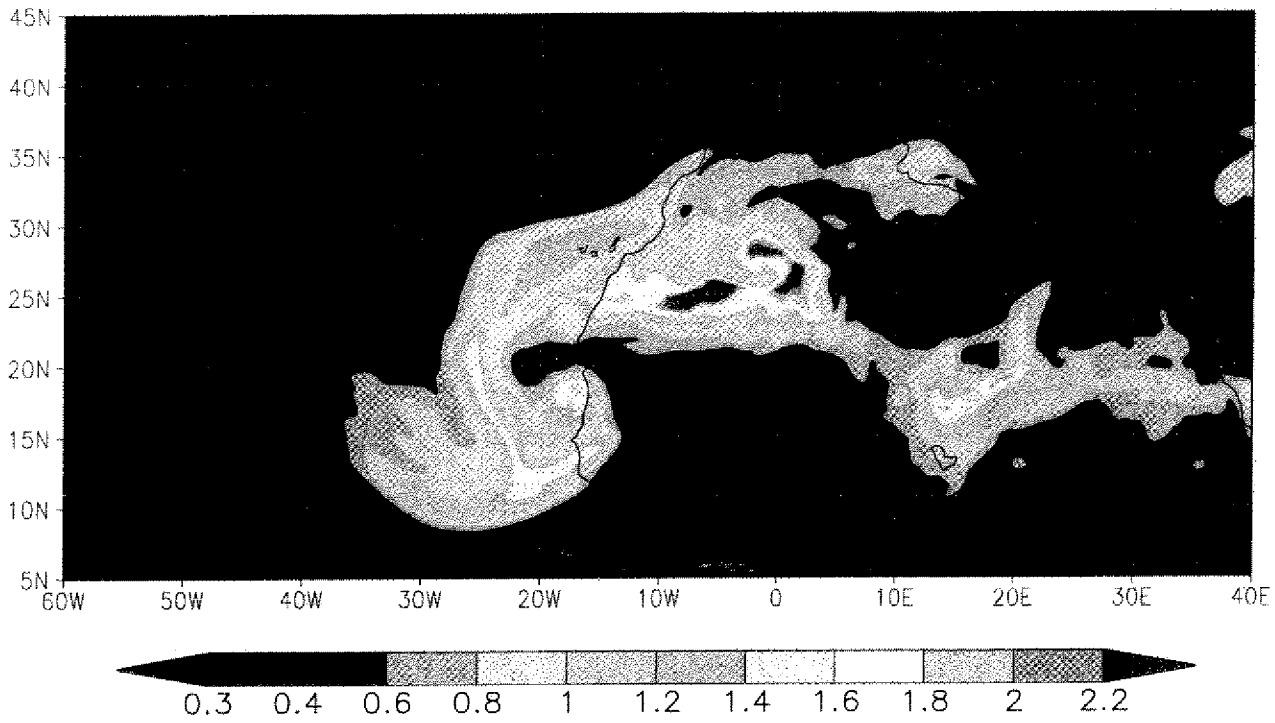
GEOS-5 In00z24Aug Ver12z25Aug 36hFc
45N
40N
35N
30N
25N
20N
15N
10N
5N
60W
50W
40W
30W
20W
10W
0
10E
20E
30E
40E
0.3
0.4
0.6
0.8
1
1.2
1.4
1.6
1.8
2
2.2

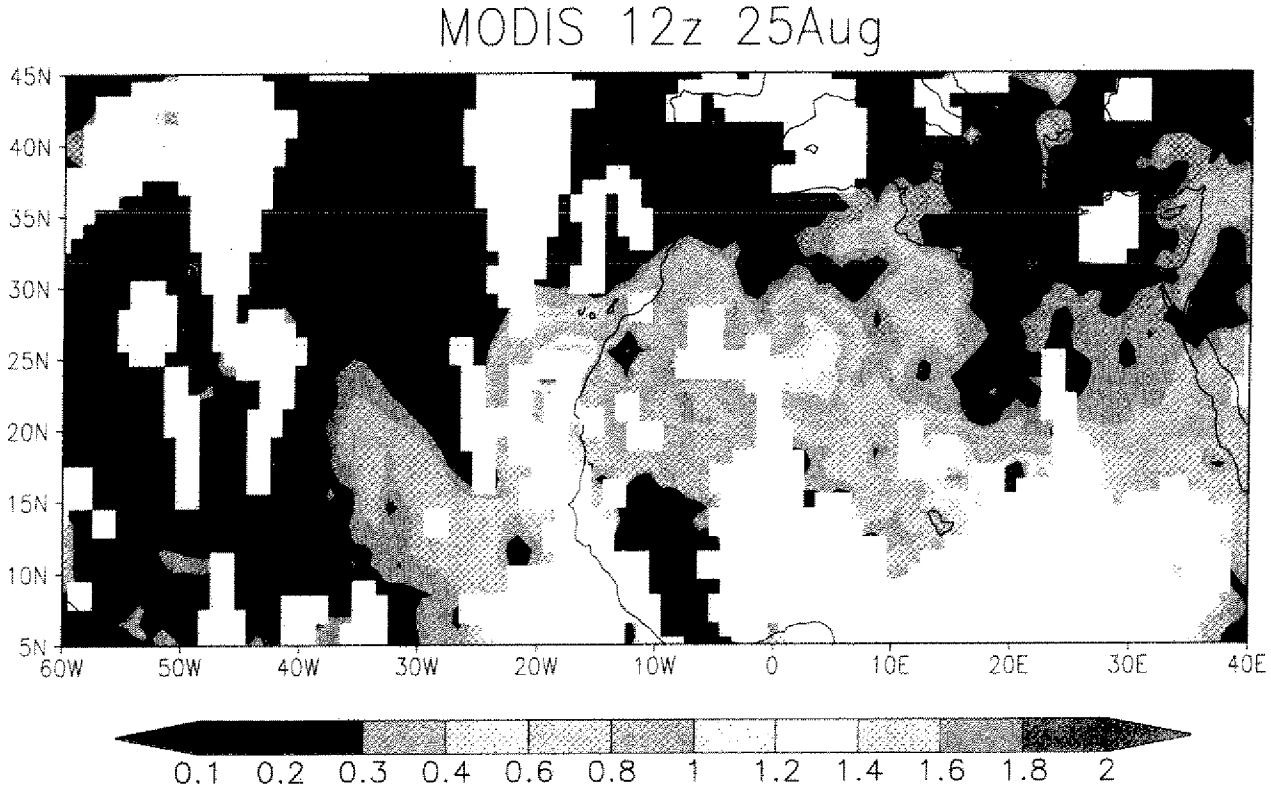
MODIS 12z 25Aug
45N
40N
35N
30N
25N
20N
15N
10N
5N
60W
50W
40W
30W
20W
10W
0
10E
20E
30E
40E
0.1
0.2
0.3
0.4
0.6
0.8
1
1.2
1.4
1.6
1.8
2

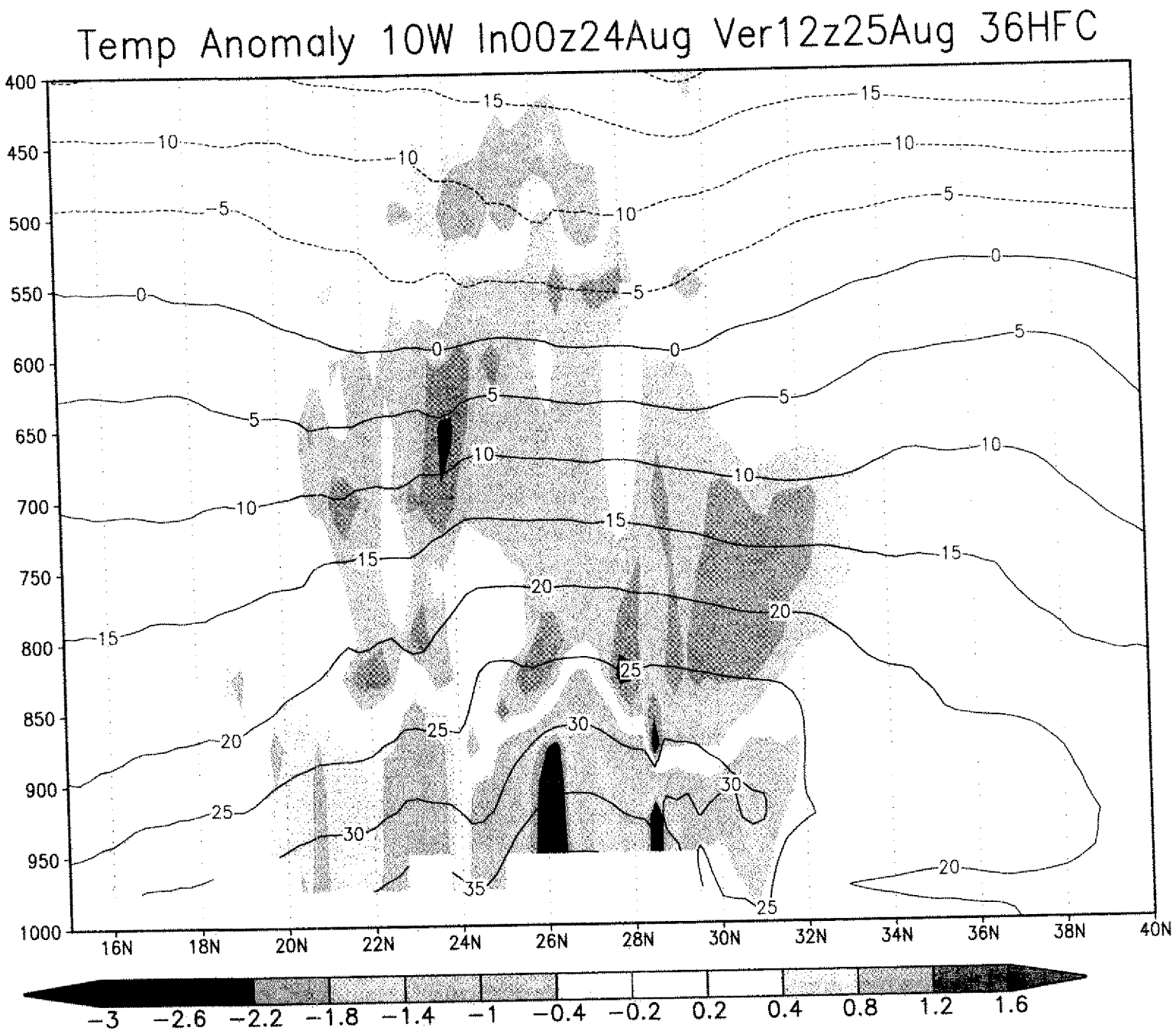
Temp Anomaly 10W In00z24Aug Ver12z25Aug 36HFC
400
450
500
550
600
650
700
750
800
850
900
950
1000
16N
18N
20N
22N
24N
26N
28N
30N
32N
34N
36N
38N
40N
−3
−2.6
−2.2
−1.8
−1.4
−1
−0.4
−0.2
0.2
0.4
0.8
1.2
1.6

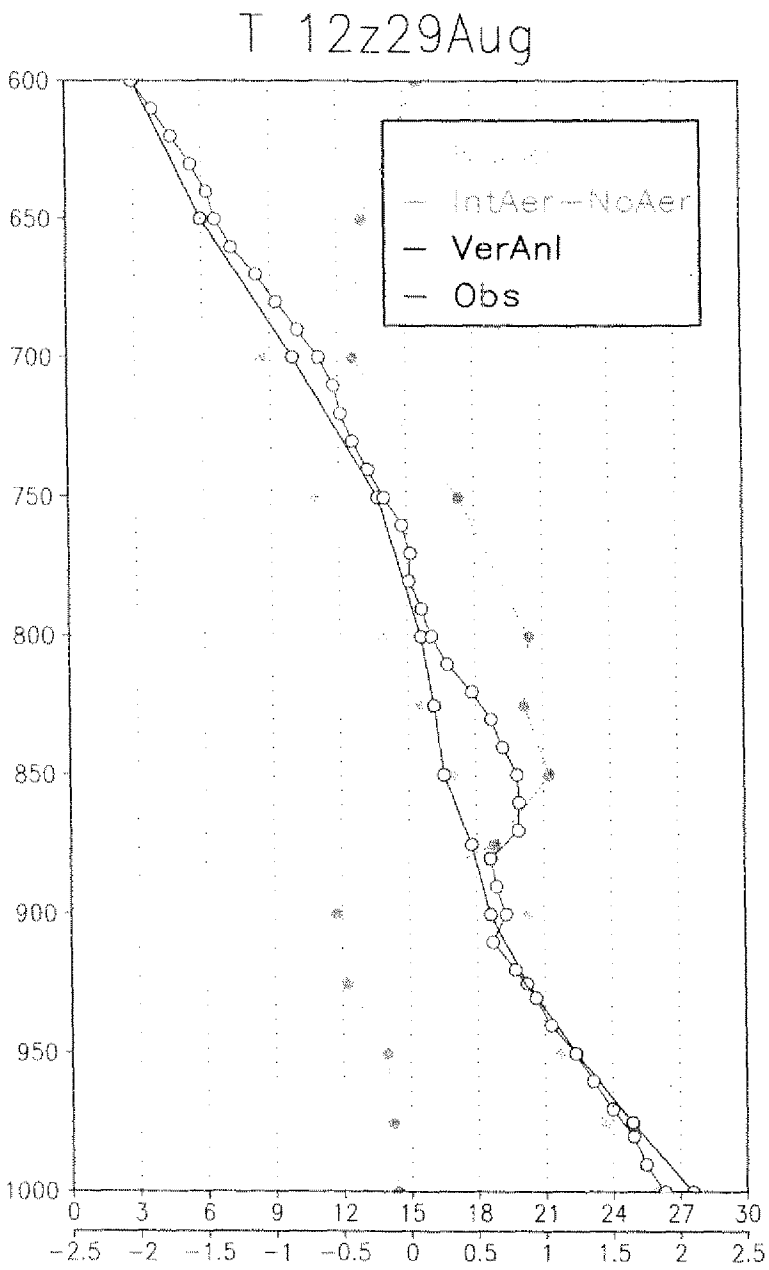
T 12z29Aug
IntAer−NoAer
VerAnl
Obs
600
650
700
750
800
850
900
950
1000
0
3
6
9
12
15
18
21
24
27
30
−2.5
−2
−1.5
−1
−0.5
0
0.5
1
1.5
2
2.5

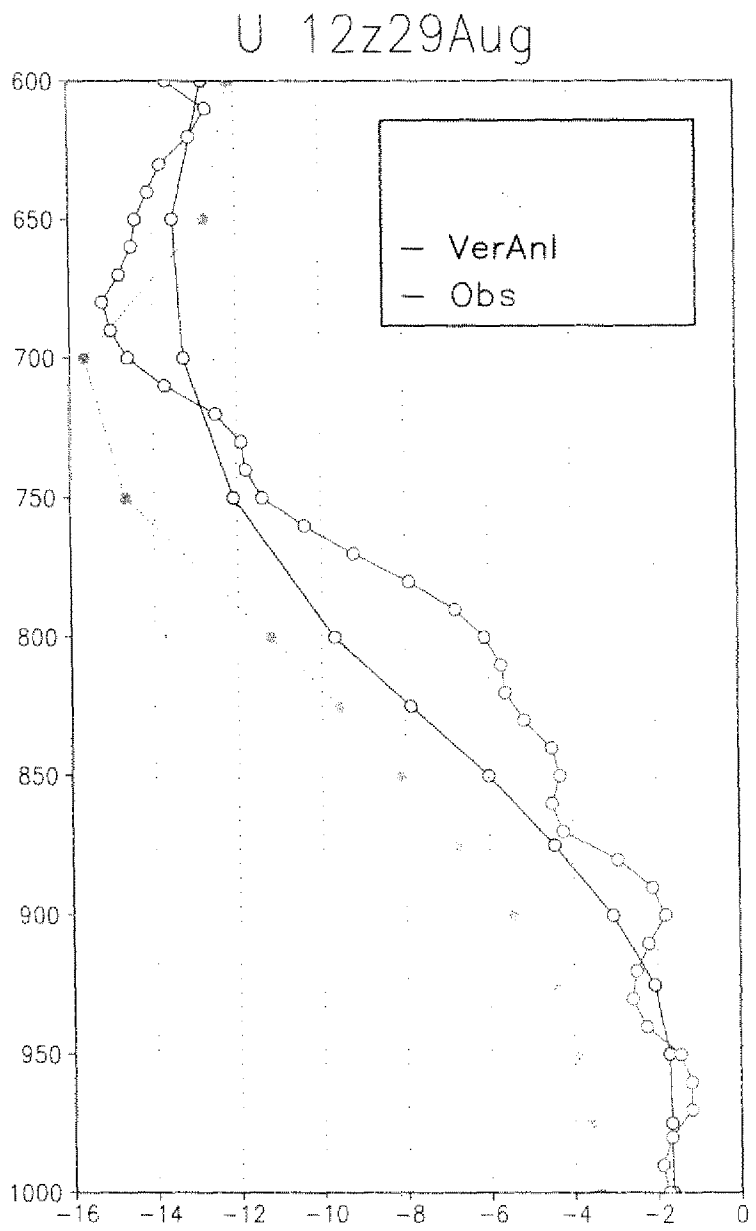
U 12z29Aug
VerAnl
Obs
600
650
700
750
800
850
900
950
1000
−16
−14
−12
−10
−8
−6
−4
−2
0